

Molecular Hydrogen and Excitation in the HII 1 -2 System

A. Noriega-Crespo¹

Infrared Processing and Analysis Center, California Institute of Technology, JPL,

Pasadena, CA, 91125

Electronic mail: alberto@ipac.caltech.edu

P. M. Garnavich

Dominion Astrophysical Observatory, Herzberg Institute of Astrophysics, Victoria, BC,

V8X 4M6

Electronic mail: pterg@dao.nrc.ca

Received _____; accepted _____

¹Part of this research was carried out at Department of Astronomy, University of Washington

ABSTRACT

We present a series of molecular hydrogen images of the Herbig-Haro 1 - 2 system in the H_2 OS(1) transition at $2.121 \mu\text{m}$, with a spatial resolution of $\sim 2''$. The distribution of H_2 is then compared with that of the excitation, given by the [sII] 6717-6731 to $\text{H}\alpha$ line ratio.

We find that most optical condensations in the HH 1 - 2 system, including the VLA 1 jet, have H_2 counterparts. H_2 emission is detected in most low excitation knots, as expected for low velocity shock S ($50 \text{ km s}^{-1} \ll S$), but also in high excitation regions, like in HH 1F and HH 2A'. For these latter objects, the H_2 emission could be due to the interaction of the preionizing flux, produced by $150\text{-}200 \text{ km s}^{-1}$ shocks, with the surrounding interstellar matter, i.e. fluorescence. The lack of fluorescent lines in the UV, however, suggest a different mechanism. H_2 is detected at the tip of the VLA 1 jet, where the knot morphology suggests the presence of a second bow shock. H_2 is detected also SE of HH 2E and SW of HH 11; in regions with known NH_3 emission.

1 INTRODUCTION

The Herbig-aro (2 system is perhaps the best studied object in its class (see e.g. Solf & Böhm 99 ; Böhm & Solf 1992 and references there in). It provides us, nevertheless, with a wealth of information on the structure of bipolar outflows, their interaction with the surrounding medium, and the latest stages of star formation (see e.g. Shu, Adams & Lizano 1987). 2 objects 1 and 2 are identified with the working surfaces of a bipolar outflow driven by the embedded source VLA 1 (Pravdo et al. 1985). The individual condensations that define these objects are likely to be due to thermal and dynamical instabilities in the flow (Laga et al. 1988; Blondin, Königl & Fryxell 1989). The presence of a faint optical blueshifted jet arising near VLA 2, plus the proper motions of the condensations, including those from HH 1 - 2, agree with the bipolar outflow scenario (Herbig & Jones 1981; Rodríguez et al. 1990; Reipurth et al. 1993; Mislöf, Mundt & Böhm 1994).

The spectra of HH objects arise in the recombination regions behind shock waves (Schwartz 1975), which are the result of the supersonic interaction of the outflowing stellar/disk material with the circumstellar medium. According to their spectra 2 objects have been classified as low and high excitation (see e.g. Dopita 1978; Böhm, Krugel & Mannery 1980, Böhm, Krugel & Ohmsted 1983). High excitation objects have strong [O II] emission, relative to He I or H β , due to shock velocities $> 80 \text{ km s}^{-1}$, with less strong [S I] and weak [N I] and [C I] lines. Low excitation objects have bright [N II], [C I], [O I] and [S I] lines, and no [O II] emission, indicating shock velocities $\leq 60 \text{ km s}^{-1}$ (see e.g. Böhm & Solf 1990). At shock velocities $40 < \text{km s}^{-1}$ an important fraction of the total emission is released at infrared wavelengths from molecular rotational-vibrational transitions of 2. CO and H $_2$ O, as well as from atomic and ionic fine structure (forbidden) transitions, e.g. [Fe I] 1.64 μm , [O I] 63 μm , [C II] 57 μm and [Si I] 35 μm (see e.g. Hollenbach & Meeker

1989).

1111 objects have been observed in the NIR spectroscopically and with narrow band imaging, particularly around the $v = 0 - 1$ $S(1)$ $2.12\mu\text{m}$ H_2 emission line which can be quite strong (see e.g. Schwartz, Cohen & Williams 1987). Some of the most recent work includes III 1 - 2 (Elias 1980; Zinnecker et al. 1989; Zealey et al. 1992); III 7- 11 (Garden, Russell & Burton 1990; Stapelfeldt et al. 1991; Curie 1992; Carr 1993), III 46/47 (Zealey, Sutters & Randall 1993; Eislöffel et al. 1994), III 90/91 (Gredel, Reipurth & Heathcote 1992), and III 111 (Gredel & Reipurth 1993). Models of the H_2 and HCO^+ emission from working surfaces in relationship to 1111 objects (Wolfire & Königl 1991, 1993; Curie 1992) suggest the presence of at least another 3 possible mechanisms to produce H_2 emission, besides collisions excitation (in dissociative and nondissociative shocks). For each case the ratio of $2 - 1 S(1)$ to $1 - 0 S(1)$ plus presence or absence of IR, UV lines and continuum give a diagnostic of the region and the process where the emission is formed. H_2 can be excited as well by entrainment (Ismailović et al. 1994) and/or by shocks with a magnetic precursor (Draine & Roberge 1982; Hartigan, Curie & Raymond 1989), with the net result that is difficult to interpret uniquely the origin of the H_2 emission.

Ideally, in order to understand the nature of III objects, we would like to address the following questions: What mechanisms give rise to the molecular emission in Herbig-Haro objects and jets? What is the correlation between excitation (a measurement of the shock characteristics and strength) and the molecular emission? As a preliminary step in this direction, we present a series of H_2 images taken at $2.121\mu\text{m}$ of the III 1 - III 2 region, and we compare them with maps of their excitation (an indicator of the shock properties) measured by the ratio of the $[S II] 6717/31$ to $\text{H}\alpha$ line ratio. The H_2 images are better defined than those previously published (see e.g. Zealey et al. 1992), and display some new interesting features. In section § 2 we describe the observations; in § 3 we discuss the results, and we summarize the main points in § 4.

2. Observations

We obtained near-infrared images of III 1 - 2 over two nights in October 1992 using the GRIM infrared imager at the Apache Point Observatory. At that time, a temporary 1.8m diameter primary mirror was in place, awaiting the compaction of the 3.5m mirror. The IR detector was a HgCdTe 128×128 array, with a scale of $\sim 0.72''$ at $f/5$. There was a warm region at the south-west corner of the detector which increased the noise and made flat-fielding there difficult. The resolution for the images is $\sim 2''$, with a field of $\sim 1.5'$. Images were taken through two filters. The first, a 25 nm wide filter centered at $2.12\mu\text{m}$ contains the molecular hydrogen transition $v=1-0$ S(1) within its bandpass. The second filter was 80 nm wide, centered at $2.22\mu\text{m}$ and was used to estimate the continuum. We note, however, that the "continuum" filter may also contain an unknown contribution from the molecular hydrogen transition $v=1-0$ S(0). The ratio of $2.22\mu\text{m}$ to $2.12\mu\text{m}$ flux ranges from 0.2 to 0.6 depending on the excitation mechanism (notice that Noriega-Crespo & Garnavich (1994) found a ratio of 0.4 in the III 1A region). Since the normalization factor of the continuum bandpass is ~ 3 , we expect errors in the measured $2.12\mu\text{m}$ flux of $\sim 10-20\%$. Eight images of III 1 were obtained in each filter, and the telescope shifted by approximately 20 arcseconds between exposures. Four exposures per filter were taken of III 2. The exposure time was 300s in the $2.12\mu\text{m}$ filter and 180s in the continuum band. Flat-field frames were obtained in a nearby region devoid of bright stars. The individual data frames were dark subtracted and flat-field corrected using the IRAF IMRED package. Stars in the III 1-1 frames were measured and the images shifted to a common pixel coordinate system before being averaged. The III 2 frames contained no stars, so the images were registered using the brightest three knots of emission.

The IR standard III 1160 (Elias et al. 1982) was observed in both filters in order to determine the relative amount of continuum transmitted by the filters. The off-band frames

were corrected by a factor of 3.05 to account for the passband differences, and then the combined $2.22\mu\text{m}$ image was subtracted from the averaged $2.12\mu\text{m}$ frame to produce the final images of molecular hydrogen.

We also used some optical images taken with two narrowband filters centered at $[\text{S II}]6717/31$ and $\text{H}\alpha$ 6563 \AA , in order to compare the optical emission and excitation with that of the H_2 . The optical images were taken with the 3.5m ESO NTT telescope and their analysis has been published elsewhere (see Reipurth et al. 1993, for details).

3. Results and Discussion

The essential spectroscopic and dynamical properties of the HH 1-2 flow are well known (although not necessarily understood!). The leading working surfaces, HH 1 and 2, are moving near the plane of the sky with tangential velocities $\geq 200 \text{ km s}^{-1}$. The VLA 1 jet tangential velocities range from $\sim 100 \text{ km s}^{-1}$ near the source to $\sim 350 \text{ km s}^{-1}$ farther away from it (Eislöffel, Mundt & Böhm 1994), which is as high as that of HH 113, and these are the highest tangential velocities measured in the outflow. Spectroscopically, based on the presence of $[\text{O III}]$ emission, HH 1 and 2 are, broadly speaking, high excitation objects. The VLA 1 jet lacks $[\text{O III}]$, but is bright in $[\text{S II}]$ and $[\text{O I}]$, and therefore, is considered a low excitation object (see e.g. Solf & Böhm 1991). Detailed comparison of the spectra with shock models (see e.g. Dopita 1978; Shull & McKee 1979; Hartigan, Raymond & Hartmann 1987) gives values of $\sim 100 \text{ km s}^{-1}$ shock velocities for HH 1 and 2; and $\sim 20 - 40 \text{ km s}^{-1}$ for the VLA 1 jet. For a determination of the shocks models is necessary *a priori* knowledge of the preshock conditions, which implies that several assumptions are made. Nevertheless, it is possible to show that large $[\text{S II}]$ to $\text{H}\alpha$ line ratios indicate low excitation and shock velocities, while the opposite is true for high excitation. We chosen in this work to separate between high and low excitation among *individual* condensations by

using values of $[S II]/H\alpha > 1$ for the low excitation and $1 <$ for the high.

3.1. III 1

III 1 can be modeled in many of its properties as a bow shock that plunges into its surrounding medium with $V_{shock} \geq 100 \text{ km s}^{-1}$ (see e.g. Noriega-Crespo, Böhm & Raga 1989). Shock models including H_2 indicate that for velocities $\geq 50 \text{ km s}^{-1}$, the molecular hydrogen is dissociated. Models of the H_2 emission in bow shock-like structure (Curiel 1992; Smith, Brand & Moorhouse 1991), indicate that for a bow shock velocities which exceed $30\text{--}50 \text{ km s}^{-1}$, the molecular emission is shifted from the “head” of the bow shock towards the “wings”, where the shock velocities are lower. A similar result is clearly observed in numerical simulations of working surfaces of atomic jets striking molecular circumstellar matter (Itsua 1994, private communication).

In III 1, therefore, the H_2 emission should arise at the “wings”, in the wake of condensation III 1 F, i.e. where condensations III 1A and III 1G are found (Herbig & Jones 1981). Our images (see Fig 2a) partially confirm this picture; III 1A (SE of F) shows strong and extended H_2 emission, while the III 1G (SW of F) is invisible. This is puzzling since both “wings” (see Fig 1) are visible in $[S II] 6717/31$ (although III 1G is not very bright), and extinction effects should decrease at longer wavelengths. This asymmetry is also seen in NIR spectroscopy, where the $[Fe II] 1.25\mu\text{m}$ and $1.644\mu\text{m}$ emission lines are clearly detected in III 1A and III 1G, but presence the molecular hydrogen is confined to III 1A (Noriega-Crespo & Garnavich 1994), which suggests a density difference between these regions (Zealey et al. 1992).

Somewhat surprising is the detection of III 1F in molecular hydrogen (see Fig 2a). Given our spatial resolution, the superposition of high excitation with the H_2 image indicates that their centroids coincide. Since III 1 F shock velocity is $\geq 100 \text{ km s}^{-1}$ (Noriega et

d. 1989) a possible mechanism for its H_2 emission is fluorescence excited by its preionizing flux (see e.g. Wolfire & Königl 1991). The excitation process of H_2 in III 1 F, however, could be more complex since the analysis of its UV emission with *IUE* does not reveal any of the features expected from fluorescence in the UV lines or the continuum (see e.g. Böhm, Noriega-Crespo & Self 1993). Another possibility requires a C-shock with a magnetic precursor (see e.g. Draine & McKee 1993). A magnetic precursor accelerates the molecules to large velocities without dissociation taking place. Present theoretical models seem to work well up to $\sim 50 \text{ km s}^{-1}$, however, this velocity is at least a factor 2 smaller than the deduced S110Cl velocity in III 1 F.

Another interesting feature in the III 1 F region is a H_2 clump one arcmin SW of III 1 F, which was previously detected in NH_3 and H_2O (Torrelles et al. 1993). We determine an approximated position of, $\alpha(1950) \sim 5^{\text{h}} 33^{\text{m}} 53^{\text{s}}$ and $\delta(1950) \sim 6^\circ 47' 11''$ (see Table 2), very close to what has been obtained using VLA, $\alpha(1950) = 5^{\text{h}} 33^{\text{m}} 53.^{\text{s}} 02$, $\delta(1950) \sim 6^\circ 47' 13.^{\text{s}} 5$ (Torrelles et al. 1993). Although it has been argued a dynamical connection between III 1 F and this clump (see e.g. Davis, Dent & Bell Burnell 1990), there is no clear physical link in H_2 emission to support this.

There are also a number of faint, red, unresolved sources that appear to be background stars (see Fig 4). Their positions are given in Table 2 with the hope that they may be used to measure the proper motion of III 1 in the IR.

3.2. VLA 1 JET

It is expected from theoretical models that in low velocity (excitation) shocks the H_2 emission should be quite strong (see e.g. Curiel 1992). Somewhat surprisingly, despite their low excitation, very few optical jets have been detected in H_2 . Among those are the chain of objects forming III 7 - 11 (Stapelheldt et al. 1991; Hartigan, Curiel & Raymond

1989; Curiel 1992; Carr 1992), 1111 46/47 (Eislöffel et al. 1994) and 1111 111 (Gredel & Reipurth 1993). It is very interesting, therefore, that the VLA 1 jet in the 1111 1-2 system is detected in H_2 . In our [S II] 6717/31 and $\text{H}\alpha$ images it is possible to distinguish nearly 8 condensations or knots along the jet. (see e.g. Reipurth et al. 1993). In the H_2 images we discern about 7 condensations. At first glance the superposition of the optical and H_2 images match quite well, except for one knot (see Mow). We tried to perform a more careful analysis of the jet knots positions for two reasons: i) search of large offsets between the optical and IR images, and ii) to see how close to the source the H_2 emission could be detected. If the knots or condensations were due to *internal* working surfaces created by variability of the source (see e.g. Raga 1993, and references therein), for instance, the H_2 emission wouldn't coincide with its optical counterpart (Curiel 1992). And since the $2.12\mu\text{m}$ emission is less affected by extinction than the optical, there is the possibility to search for the jet closer to the source.

There are many caveats, however, in measuring the H_2 knots positions. The image resolution is not excellent, neither is the signal-to-noise, and there are not enough stars in our frames to do the best astrometry. We can do little about the first two problems (except to get more observing time), but for the last problem is possible to assume that optical of the [S II] and H_2 condensations coincide in their positions. For the VLA 1 jet, we have taken till now positions as known: the Cohen-Schwartz Star, H11P and the lateral knot 1111 1 11B (Reipurth et al. 1993). The measured positions for the [S II] and H_2 frames are shown in Table 1 (we used nomenclature from Reipurth et al. (1993)). The positions are remarkable similar, with the only exception perhaps of the 'jet A' condensation, i.e. neither we measured offsets nor we detected H_2 closer to the source.

The condensation 'jet A' at the upper tip of the jet, however, deserves a little bit more attention. It is a better delineated knot than its [S II] counterpart and northward. Enlargement of the image reveals an almost bow shock-like structure (See Fig 3a,b), similar

to what it is observed optically in other Herbig-Haro jets, e.g. HH 111 (Reipurth 1989), HH 34 (Reipurth & Heathcote 1992), and HH 46/47 (Hartigan et al. 1993). Multiple bow shocks are expected to appear when the outflow from the driving source changes with time (see e.g. Raga et al. 1990). Although the extinction is probably larger in this region, which explains why the optical jet becomes invisible, the H_2 emission could be due to a different process. If this condensation were another bow shock it could have a shock velocity $\sim 50 - 100 \text{ km s}^{-1}$ (recall that the jet itself is moving at $\sim 350 \text{ km s}^{-1}$ in that region (Fisloff et al. 1994)), and once again it is tempting to invoke a C-shock with a magnetic precursor, to preserve the molecular hydrogen.

Given the low excitation of the jet, the shocks involved are weak and unable to generate large post shock densities, and therefore, enough H_2 column density to explain the observations. This means that the observed H_2 is already there when the jet strikes. Although another possibility is that entrainment of the surrounding molecular material is taking place, as it seems to be the case in HH 46/47 (Hartigan et al. 1993).

3.3. HH 2

The morphology of HH 2 (see Fig 2b) is more complex than that of HH 1 (see e.g. Schwartz et al. 1993), and although broadly speaking it resembles a bow shock structure, the excitation, velocity dispersion and proper motion of its condensations does not follow a simple bow shock model (see e.g. Böhm & Solf 1992). It is interesting, therefore, to find that there is a good correspondence between the optical and molecular emission, for at least half of the condensations (see Figs 3c,d). In detail we can associate H_2 features to the following condensations: A, B, D, E, F, G, J, K and L. The brightest condensation, H, and the faint one, I, are hardly detectable. The H_2 emission farther downstream (N of A) fades

away very rapidly, where condensations O, P, Q, R, S and '1' are found, although there is still a trace of emission.

The very high excitation condensation 11 lacks of a well defined counterpart in the H_2 emission, but there is some faint trace, which it could be arising from behind f] and/or ahead of condensation A'. This later one, of intermediate excitation, has a bright H_2 'core' and an extended emission region (Fig 3c), although, as in the case of III 1F, it is difficult to explain unless an efficient reformation of H_2 takes place behind its shock, since there is no evidence of fluorescent H_2 in that region from UV observations (Böhm et al. 1993).

We notice as well a small bright knot NE of condensation L without an optical counterpart (Fig 3d). This condensation seems to have a NH_3 counterpart, however, (Torrelles et al. 1992) and it may be unrelated to the III 2 flow.

4. CONCLUSIONS

We presented a series of images in $v = 1 - 0 \text{ S}(1) 2.12 \mu\text{m}$ light of the III 1 - 2 region, with better resolution than previous images (Zealey, Sutters & Randall 1993; Zealey et al. 1992). We compared the H_2 images with maps of their excitation measured by the $[\text{S II}] 6717/31$ to $\text{H}\alpha$ line ratio.

We found that at least half of the optical condensations in III 2, as well as III 1F and III 1A, plus most of the VLA 1 jet knots have H_2 counterparts at similar positions within our resolution. Most of these objects have a lower excitation, with the exception of condensations III 1 F and III 2A' which have a higher excitation. For these latter objects, the lack of fluorescent emission in the UV (Böhm et al. 1993), suggests a different H_2 excitation mechanism, and it may require the reformation of the H_2 molecules behind the shock and farther downstream (Wolfire & Königl 1991).

In the VLA 1 jet the NW tip in H_2 dots not have a clear optical counterpart, and it has a 'bow shock-like' morphology. The absence of an optical counterpart may be explained by the increment of the extinction in this region or by a 'density' effect (as in the NW wing of 1111 1). There is the possibility, however, that this knot may be tracing a second outburst, in which the material is being excited by a 'magnetic precursor'. Spectroscopic observations should determine if this is the case, based on the width of the 1σ lines. The high excitation condensation 1111 11 (with $v_{shock} \sim 100 - 200 \text{ km s}^{-1}$) may also require a C-type shock to explain its emission, since as mentioned above, no evidence of fluorescence has been found in the UV. It is appealing to talk about a C-type shock with a magnetic precursor, because such process accelerates the molecules at high velocities without dissociating them, although for $B \sim 1 \text{ mG}$, a shock with $v_{shock} \sim 50 \text{ km s}^{-1}$ dissociates most of the H_2 (for a review see e.g. Draine & McKee 1993).

Finally, condensation III 211, which it has a very high excitation, dots not show an obvious molecular hydrogen counterpart. The trace of emission (Fig 3c,d) ahead of III 2A' could, however, be associated with it. We notice that similar results have been recently reported (Davis, Eisloffel & Ray 1994), and that H_2 images with a higher resolution show positional offsets with respect the $[S II]$ and $H\alpha$ emission in 11112.

A.S. - C. research has been supported by NSF grant AST-91-14555, through the Department of Astronomy at University of Washington, & NASA Long Term Space Astrobiology's Program through a contract with the Jet Propulsion Laboratory of the California Institute of Technology. We thank Bo Reipurth and Steve Heathcote for providing us with the $[S II]$ and $H\alpha$ NTT images, and the anonymous referee for her/his careful reading of the manuscript. GRIM is working thanks to Mark Hereld and his team, and we are grateful to them.

Figure 1. Grayscale (linear) map of the HH 1 - 2 region based on a narrow band (CC) image centered at [S II] λ 671 7/31 emission lines (from Reipurth et al. 1993). The Cohen-Schwartz (C-S) star, the VLA1 source and some of the brightest condensations are indicated.

Figure 2a. An H₂ image at 2.12 μ m of the HH 1 object including the VLA1 jet. The superimposed contour lines correspond to the [S II] 671 7/31 emission. Most bright H₂ knots have optical counterparts, except for a bright knot SE of the C-S star and along the line joining to VLA 1 source, for which an optical counterpart is not detected. The field is $\sim 1.3'$ and N is up.

Figure 2b. As above, but for the HH 2 region. Notice the small bright knot NE of condensation L without an optical counterpart.

Figure 3a. A comparison between the H₂ molecular emission and the LOW excitation ([S II]/H α > 1) emission for the VLA 1 jet and HH 1 (contour lines).

Figure 3b. H₂ molecular emission and the H₂ excitation ([S II]/H α < 1) emission for the VLA 1 jet and HH 1.

Figure 3c. H₂ molecular emission and the LOW excitation ([S II]/H α > 1) emission for HH 2.

Figure 3d. H₂ molecular emission and the H₂ excitation ([S II]/H α < 1) emission for HH 2.

Figure 4. CCD image of the sum of the 2.12 μ m and 2.22 μ m flux of the HH 1 region where some of the 'background' stars and objects are marked (see Table 2). The field is $\sim 1.3'$ and N is up.

REFERENCES

- Blondin, J.M., König, A, & Pyxel, B.A. ApJ 117, 37
- Böhm, K.J., Prugel, E.W., & Mannery, E. 1980, ApJ, 235, L17
- Böhm, K.J., Prugel, E.W., & Olmsted, B. 1983, A&A, 125, 23
- Böhm, K.J., & Solf, J. 1990, ApJ, 348, 297
- Böhm, K.J., & Solf, J. 1992, AJ, 104, 1193
- Böhm, K.J., Noriega-Crespo, A., & Solf, J. 1993, ApJ, 406, 647
- Cart, J. 1993, ApJ, 406, 553
- Curiel, S. 1992, PhD Thesis, Universidad Nacional Autónoma de México
- Davis, C.J., Dent, W.R.F., & Bell Burnell, S.J. 1990, MNRAS, 244, 173
- Davis, C.J., Bistöfl, J., & Ray, T.P. 1994, ApJ, (in press)
- Draine, B.T., & Koberge, W.G. 1982, ApJ, 259, 91
- Draine, B.T., & McKee, C.P. 1993, MNRAS, 31, 373
- Dopita, M. 1978, ApJS, 37, 7
- Bistöfl, J., Mundt, R., & Böhm, K.H. 1994, ApJ (submitted)
- Bistöfl, J., Davis, C.J., Ray, T.P., & Mundt, R. 1994, ApJ (submitted)
- Elias, J.H. 1980, ApJ, 241, 728
- Elias, J.H., Progel, J.A., Matthews, K., & Neugebauer, G. 1982, AJ, 87, 1029
- Garden, R.P., Russell, A.G., & Burton, M.G. 1990, ApJ, 354, 232
- Gredel, R., & Reipurth, B. 1993, ApJ 407, 229
- Gredel, R., Reipurth, B., & Catala, S., 1992, A&A, 266

- Hartigan, P., Curie], S. & Raymond, J. 1989, *ApJ*, 347, 31
- Hartigan, P., Morse, J. A., Heathcote, S., & Cecil, G., 1992, *ApJ*, 414, 1,121
- Hartigan, P., Raymond, J., & Hartmann, L. 1987, *ApJ*, 316, 323
- Hartigan, P., Morse, J. A., Heathcote, S., & Cecil, G. 1993, *AJ*, 414, 1,121
- Herbig, G.H. 1974, *Lick Obs Bull*, 658
- Herbig, G.H., & Jones, B.F., 1981, **AJ**, 86, 1232
- Hollenbach, D. J., & McKee, C.F. 1989, *ApJ*, 342, 306
- Noriega Crespo, A., Böhm, H. J., & Raga, A.C. 1989, *AJ*, 98, 1388
- Noriega-Crespo, A., & Garnavich, P.M. 1994, *RMxAA* (submitted)
- Pravdo, S.J., Rodríguez, L.F., Curiel, S., Cantó, J., Torrelles, J. M., Becker, T.T., & Sellgren, K., 1985, *ApJ* **m**, 1,35
- Raga, A.C., Matco, M., Böhm, K.H., & Self, J. 1988, *AJ*, 95, 1783
- Raga, A.C., Cantó, J., Binette, L., & Calvet, N. 1990, *ApJ*, 364, 601
- Raga, A.C. 1993, *ASpSc*, 208, 163
- Raymond, J.C., Morse, J.A., Hartigan, P., Curiel, S., & Heathcote, S. 1994 in "Stellar and Circumstellar Astrophysics", eds G. Wallerstein & A. Noriega-Crespo, ASP Series, 57, p53
- Reipurth, B. 1989, *Nature*, 340, 42
- Reipurth, B., & Heathcote, S. 1992, *A&A*, 257, 693
- Reipurth, B., Heathcote, S., Roth, M., Noriega-Crespo, A. & Raga, A.C. 1993, *ApJ*, 408, L19
- Rodríguez, L.F., Ho, P.T.P., Torrelles, J.M., Curiel, S., & Cantó, J. 1990, *Apj*, 352, 645
- Schwartz, R.D. 1975, *ApJ*, 195, 631

- Schwarzs, R.D., Cohen, M., & Williams, P.M., 1984. *ApJ*, 322, 403
- Schwartz, R.D., Cohen, M., Jones, J.J., Böhm, K.I., Raymond, J.C., Hartmann, L., Mundt, R., Dopita, M.A., & Shultz, A.S. 3. 1993, *AJ*, 106, 740
- Shu, F.H., Adams, F.C., & Lizano, S. 1987, *MNRAS*, 25, 1
- Shull, M. & McKee, C.F. 1979, *ApJ*, 227, 131
- Smith, M.D., Brand, P.W.J., & Moorhouse, A. 1991, *MNRAS*, 248, 451
- Solf, J., & Böhm, K.I. 1991, *ApJ*, 375, 618
- Stappelfeldt, K.R., Reichman, C.A., Hester, J.J., Scoville, N.Z., & Gautier, T.N.. 11, 1991, *ApJ*, 371, 226
- Strom, S.E., Strom, K.M., Grasdalen, G.L., Seligren, K., Wolff, S., Morgan, J., Stocke, J., & Mundt, R. 1985, *AJ*, 90, 2281
- Solf, J., & Böhm, K.H. 1991, *ApJ*, 375, 618
- Torrelles, J.M., Rodríguez, J.F., Cantó, J., Anglada, G., Gómez, J.P., Curiel, S., & Ho, P.T.P. 1992, *ApJ*, 396, 195
- Torrelles, J.M., Gómez, J.P., Ho, P.T.P., Anglada, G., Rodríguez, J.F. & Cantó, J. 1993, *ApJ*, 417, 655
- Wolfire, N.G., & Königl, A. 1991, *ApJ*, 383, 205
- Wolfire, N.G., & Königl, A. 1993, *ApJ*, 415, 204
- Zealey, W.J., Williams, P.M., Sandell, G., Taylor, K.N.R., & Ray, T.P. 1992, *ACSA* 262, 570
- Zealey, W.J., Suttens, M.G., & Randall, P.R. 1993, *PASA*, 10, 203
- Zinnecker, I., Mundt, R., Geballe, T.R., & Zealey, W.J. 1989, *ApJ*, 342, 337

TABLE 1. Positions¹ of VLA 1 jet knots from [S II] and H₂ images.

Object	α_{1950}	δ_{1950}	α_{1950}	δ_{1950}
jet A	5 33 56.2	6 47 37	5 33 56.1	6 47 35
jet B	5 33 56.3	6 47 41	5 33 56.3	6 47 41
jet E	5 33 56.5	6 47 46	5 33 56.5	6 47 46
jet F	5 33 56.6	6 47 48	5 33 56.7	6 47 47
jet G	5 33 56.7	6 47 49	5 33 56.8	6 47 49

¹epoch 1992

TABLE 2. Positions¹ of background and surrounding sources

Object	α_{1950}	δ_{1950}
III 1F ^a	5 33 54.54	-64657.0
C-S star ^b	5 33 55.55	-6 4725.1
1 ^b	5 33 58.08	-6 47 11.7
2	5 33 53.94	-6 4748.3
3	5 33 56.29	647 15.4
4	5 33 55.89	64728.5
5	5 33 54.74	64656.9
6 ^c	5 33 56.88	6 47 50.0
7 ^d	5 33 53.16	-64711.1
8 ^e	5 33 55.32	-64755.2

¹epoch 1992

^aFrom Herbig (1974)

^bFrom Strom et al. (1985)

^cBright continuum at the start of the VLA 1 Jet

^dH₂O maser, see Torrelles et al. (1993)

^eIII 144, see Reipurth et al. (1993)

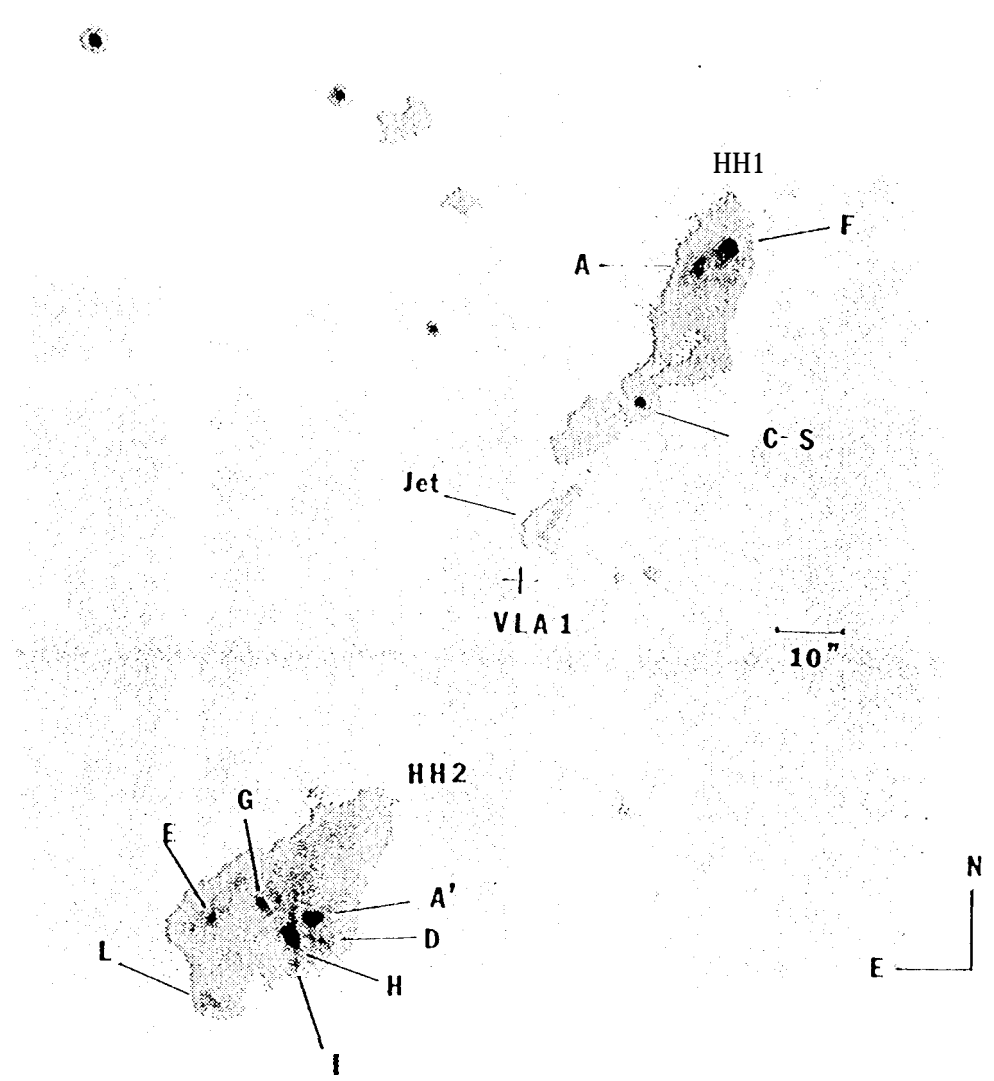


Figure 1

1980

10



Figure 2a

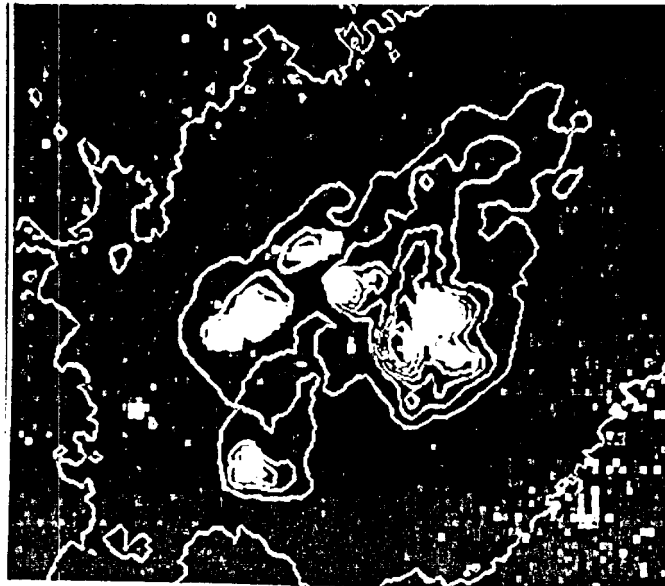


Figure 2b

A. Noriega-Crespo y P.M. Garnavim

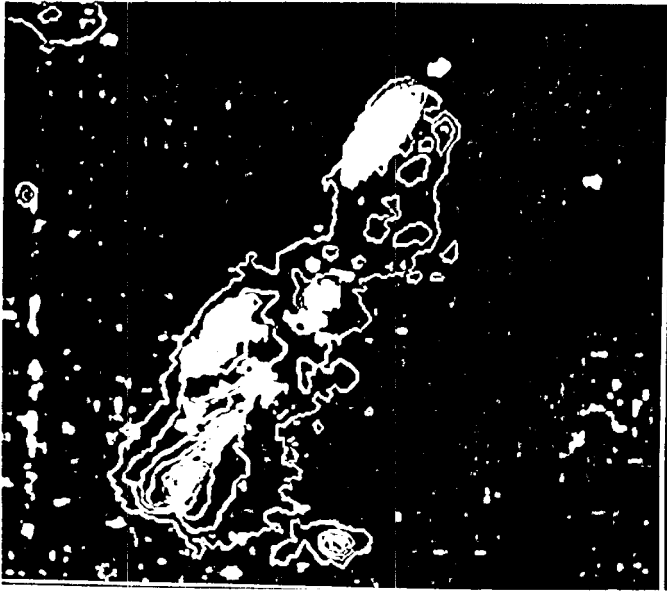


Figure 3a

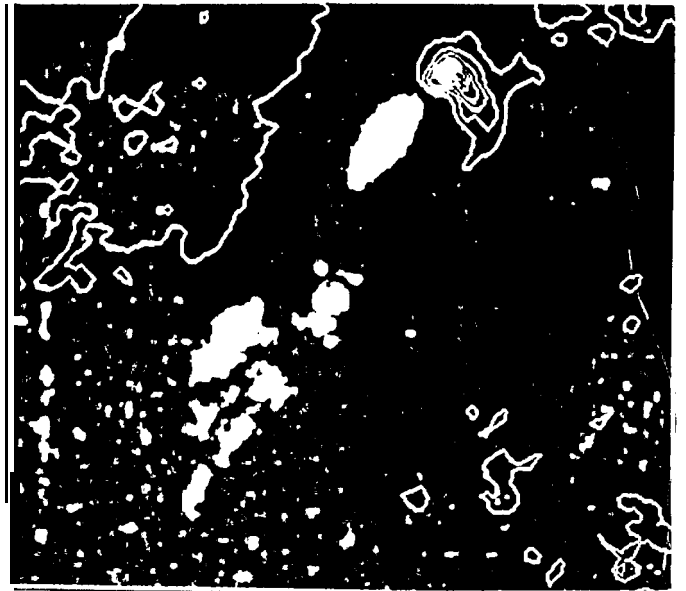


Figure 3b

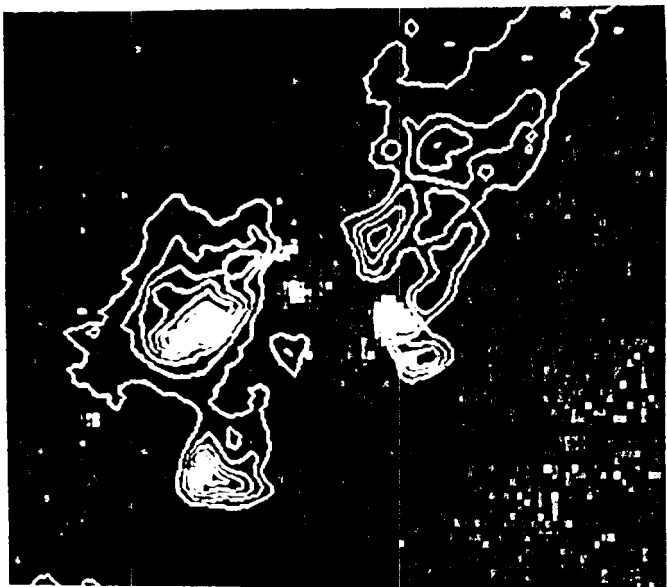


Figure 3c

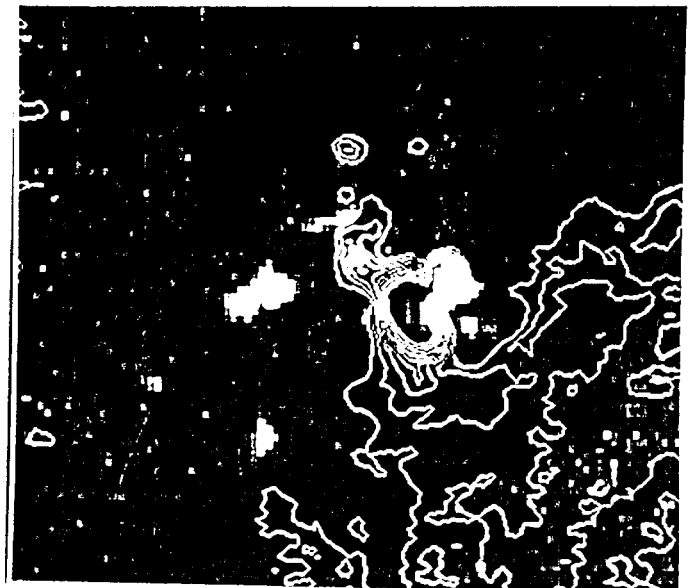
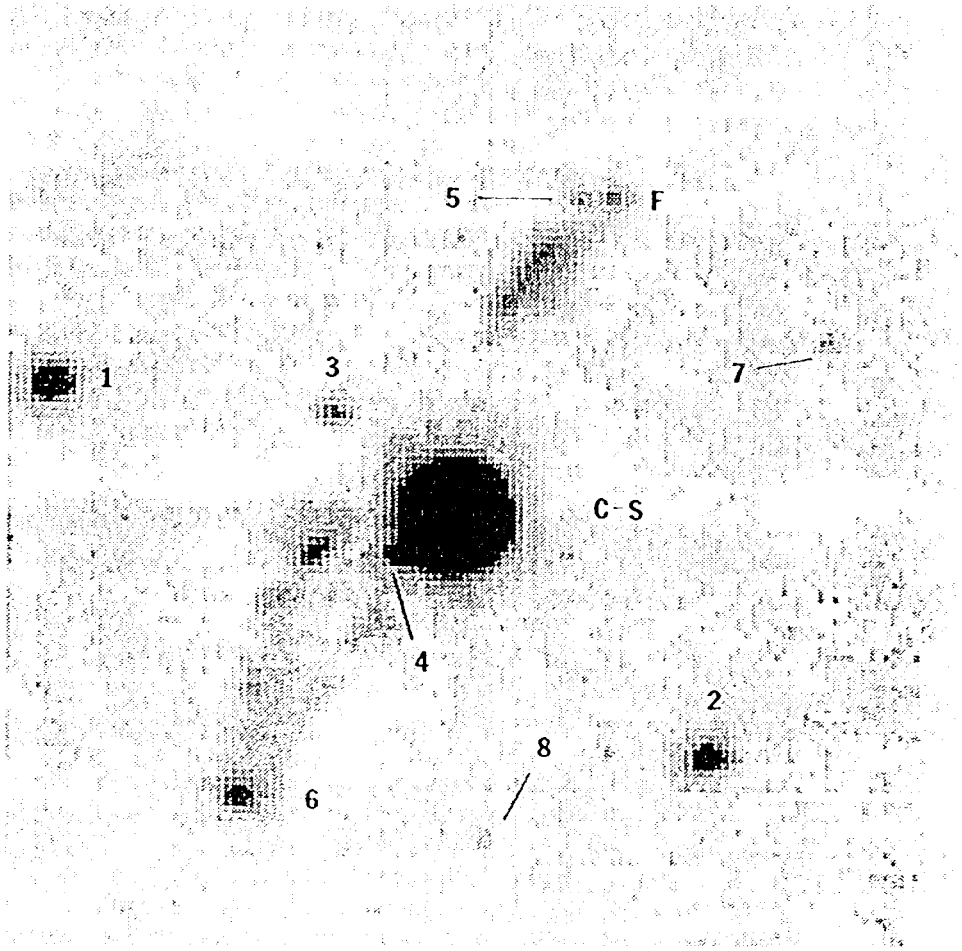


Figure 3d

A. Noriega-Crespo & P.M. Garnavich



Front
A No. 1000
1/2